Lab on a Chip

PAPER

View Article Online
View Journal | View Issue

Cite this: *Lab Chip*, 2015, **15**, 823

Integrated perfusion and separation systems for entrainment of insulin secretion from islets of Langerhans†

Lian Yi, Xue Wang, Raghuram Dhumpa, Adrian M. Schrell, Nikita Mukhitov and Michael G. Roper*

Received 17th November 2014,
Accepted 27th November 2014

DOI: 10.1039/c4lc01360c

www.rsc.org/loc

A microfluidic system was developed to investigate the entrainment of insulin secretion from islets of Langerhans to oscillatory glucose levels. A gravity-driven perfusion system was integrated with a microfluidic system to deliver sinusoidal glucose waveforms to the islet chamber. Automated manipulation of the height of the perfusion syringes allowed precise control of the ratio of two perfusion solutions into a chamber containing 1–10 islets. Insulin levels in the perfusate were measured using an online competitive electrophoretic immunoassay with a sampling period of 10 s. The insulin immunoassay had a detection limit of 3 nM with RSDs of calibration points ranging from 2–8%. At 11 mM glucose, insulin secretion from single islets was oscillatory with a period ranging from 3–6 min. Application of a small amplitude sinusoidal wave of glucose with a period of 5 or 10 min, shifted the period of the insulin oscillations to this forcing period. Exposing groups of 6–10 islets to a sinusoidal glucose wave synchronized their behavior, producing a coherent pulsatile insulin response from the population. These results demonstrate the feasibility of the developed system for the study of oscillatory insulin secretion and can be easily modified for investigating the dynamic nature of other hormones released from different cell types.

Introduction

Islets of Langerhans, are the endocrine tissue in the pancreas and respond to increased glucose levels with the release of insulin. Islets are composed of ~2000 cells with the majority of those being β-cells. Secretion of insulin from individual β-cells is pulsatile and it has been suggested that the pulsatility is due to oscillations in glycolysis mediated by the enzyme phosphofructokinase (PFK).[1,2] Within a single islet, thousands of β-cells coordinate their activity primarily through gap junctions resulting in a pulsatile insulin response.[3,4] *In vivo*, oscillations of insulin are observed with a period of ~5–10 min,[5–7] indicating that the ~1 million islets coordinate their secretion.[8] The mechanism behind this synchronization is still unknown, but oscillatory levels of insulin have been shown to be more effective than constant insulin levels for optimal action.[9] Impaired pulsatile insulin secretion is observed in individuals with type 2 diabetes and their relatives,[10,11] demonstrating the critical need to understand the underlying mechanisms of pulsatile insulin release.

One mechanism of *in vivo* islet synchronization is postulated to be due to a glucose/insulin feedback system.[12–14] In this scenario, glucose acts as a global signal to all islets initiating insulin release. The increased insulin levels then initiate uptake of the sugar, reducing glucose levels and removing the stimulus for insulin release. This reduction in insulin levels allows glucose levels to rise again, and the cycle is re-initiated. One consequence of this hypothesis is the entrainment, or forcing, of individual islets to an oscillatory glucose level resulting in a synchronized population. Small amplitude glucose oscillations have been shown to entrain oscillations in mitochondrial membrane potential, intracellular [Ca^{2+}] ([Ca^{2+}]$_i$), and NADPH in islets.[15–18] However, the effect of oscillatory glucose levels on insulin release has only been examined in a few studies.[19,20] To fully investigate the entrainment parameters of insulin secretion, it would be ideal to have an automated system that can deliver glucose oscillations to islets while measuring insulin levels in a time-resolved manner.

Oscillatory insulin secretion from perfused islets and in the portal vein have been measured by traditional offline assays, including radioimmunoassays and enzyme-linked immunosorbent assays.[21,22] These techniques have been used to resolve insulin oscillations with time resolution from seconds to minutes,[23] but the expense and labor of sample collection and processing hinder the use of these techniques

Department of Chemistry and Biochemistry, Florida State University, 95 Chieftain Way, Tallahassee, FL 32306, USA. E-mail: roper@chem.fsu.edu

† Electronic supplementary information (ESI) available. See DOI: 10.1039/c4lc01360c

for routine study of the entrainment of insulin secretion. The recent use of microfluidic electrophoretic immunoassays has provided a platform to monitor insulin secretion from on-chip cultured islets in an automated fashion.[24–28] For example, high throughput assays have been performed by multiplexing the channel network[26] and long term monitoring has been achieved by supplying fresh immunoassay reagents throughout the course of the experiment.[27] Recently, the number of hormones monitored was expanded by multiplexing the detection wavelength.[28] While these systems have been used to examine oscillations of hormone secretion with a temporal resolution as high as 6 s, the perfusion systems used have not been ideal for testing entrainment since they required manual intervention to switch between basal and stimulatory glucose levels.[25–28] Because of this requirement for user input, these perfusion systems have been used to deliver constant glucose concentrations, whereas entrainment requires time-dependent waves of glucose to be generated, more suited for an automated perfusion system.

In this work, we integrated a perfusion system capable of delivering physiological solutions to single or groups of islets with a system that allows monitoring insulin secretion from single and groups of islets. This system can produce glucose waveforms for testing entrainment of islets and has the sensitivity for monitoring insulin secretion from single islets. We demonstrate that insulin secretion from single islets can be entrained to glucose oscillations with periods ranging from 5 to 10 min. In addition, groups of islets were entrained to the same glucose wave producing synchronized insulin oscillations, similar to those observed *in vivo*. The methodology developed here is robust and can be modified for investigating cellular dynamics of other cell types.

Experimental

Chemicals and reagents

Bovine serum albumin (BSA), ethylenediaminetetraacetic acid (EDTA), ammonium hydroxide (NH_4OH), and sodium hydroxide (NaOH) were from EMD Chemicals (San Diego, CA). Dextrose was obtained from Fisher Scientific (Pittsburgh, PA). Sulfuric acid (H_2SO_4), nitric acid (HNO_3), hydrogen peroxide (H_2O_2), and hydrofluoric acid (HF) were from Avantor Performance Materials (Center Valley, PA). Cy5 monofunctional *N*-hydroxysuccinimide ester was from GE Healthcare Bio-Sciences (Piscataway, NJ). A monoclonal antibody to human insulin C-terminal (Ab) was obtained from Meridian Life Science, Inc. (Saco, ME). All other chemicals were obtained from Sigma-Aldrich (Saint Louis, MO), unless otherwise stated. Labeling of bovine insulin with Cy5 (Insulin*) was performed as previously described.[29] All buffers were prepared using ultrapure deionized water (NANOpure Diamond TM deionization system, Barnstead International, Dubuque, IA) and filtered using 0.2 μm nylon syringe filters (Pall Corporation, Port Washington, NY).

Fabrication of microfluidic devices

Microfluidic devices were fabricated in glass by conventional photolithography and wet etching as previously described.[28] Two photomasks were used, one for the fabrication of the electroosmotic flow (EOF) channels and one for the perfusion channels. The mask for the EOF channels was purchased from Digidat, Inc. (Pasadena, CA) and the mask for the perfusion channels was from Fineline Imaging (Colorado Springs, CO). Each photomask was aligned on top of a borofloat photomask blank (Telic Co., Valencia, CA) coated with a layer of AZ1500 positive photoresist and a chrome layer. After exposing with 18 mW cm^{-1} collimated UV radiation (OAI, San Jose, CA) for 16 s, the exposed photoresist and the underlying chrome were removed with AZ 400K Developer (AZ Electronic Materials Corp., Sommerville, NJ) and a chrome etchant solution (CR-7S, Cyantek Corp., Fremont, CA), respectively. A 5 : 1 : 3 (v : v : v) mixture of $H_2O : HNO_3 : HF$ was used to etch the exposed glass 6 μm deep for the EOF channels. The perfusion channels were etched 30 or 40 μm deep, depending if the device was used for single or multiple islets, respectively. The channel dimensions were measured with a P-15 stylus profilometer (KLA-Tencor, Milpitas, CA). The islet chamber and channel access holes were fabricated using a diamond-tipped drill bit, either 300 or 600 μm diameter, for single or multiple islet experiments, respectively. After removing the remaining photoresist and chrome, the etched glass pieces were cleaned in a 3 : 1 (v : v) solution of $H_2SO_4 : H_2O_2$ for 30 min, and subsequently in a 5 : 1 : 1 (v : v : v) solution of $H_2O : NH_4OH : H_2O_2$ for another 30 min at 60 °C. Finally, after rinsing, the two pieces of glass containing the perfusion and EOF channels were aligned by hand and bonded at 640 °C for 8 h. After bonding, reservoirs (IDEX, Oak Harbor, WA) were applied to the top of the device using adhesive rings (IDEX).

Isolation and culture of islets of Langerhans

Pancreatic islets were obtained from 20–40 g CD-1 male mice (Charles River Laboratories Internal, Inc., Wilmington, MA) as previously described.[30] Isolated islets were cultured in RPMI 1640 media (Mediatech, Inc., Manassas, VA) containing 10% calf serum, 100 units mL^{-1} penicillin, 100 μg mL^{-1} streptomycin, and 10 μg mL^{-1} gentamicin at 37 °C with 5% CO_2. The islets were used within 4 days after isolation.

Perfusion system

A balanced salt solution (BSS) was used for perfusion and was composed of 125 mM NaCl, 5.9 mM KCl, 1.2 mM $MgCl_2$, 2.4 mM $CaCl_2$, 25 mM tricine, and 1 mg mL^{-1} BSA, adjusted to pH 7.4 with 1 M NaOH. Two 60 mL plastic syringes were used to hold the perfusion solution, BSS containing 3 or 13 mM glucose. Tygon tubing (0.03 in. o.d., 0.01 in. i.d., Cole-Parmer, Vernon Hills, IL) was used to connect the syringes to the perfusion inlets on the microfluidic device through fingertight fittings (IDEX). Both syringes were mounted on a gravity driven flow system as previously

described.[15,31] The height of the syringe containing 13 mM glucose was controlled by a stepper motor (Phidgets, Calgary, Alberta, Canada) using a program written in LabVIEW software (National Instruments, Austin, TX). The syringe containing 3 mM glucose was moved in an equal and opposite direction by attaching it to the 13 mM glucose syringe with a belt and pulley (SDP/SI, New Hyde Park, New York). The ratio of these two solutions entering the perfusion mixing channel dictated the final glucose concentration delivered to the islet chamber. This ratio was determined by the ratio of the flow rates from the two syringes. The flow rate as a function of syringe height was calibrated daily through the use of 100 nM fluorescein that was added to the 13 mM glucose perfusion solution.[31] Briefly, the calibration was performed by first identifying the heights corresponding to mixing ratios beyond 100% and 0% as determined by the amount of fluorescein entering the perfusion mixing channel. The mixing ratio of the two solutions was then monitored using the fluorescence signal prior to the islet chamber while the syringes were varied between these two extremes. The fluorescence as a function of the syringe heights produced a linear curve that could then be used to produce any mixing ratio required. A more detailed description of the perfusion calibration is provided in the (ESI†), Fig. S1, and Movie S1.

Injection and detection on microfluidic device

The microfluidic device was placed on the stage of a Nikon Eclipse TS-100 inverted fluorescence microscope (Nikon Instruments, Inc., Melville, NY). A flow gated injection scheme was utilized to inject sample into the separation channel.[32] During the entire experiment, the Insulin*, Ab, and the islet reservoirs were held at ground and −5000 V was applied to the waste reservoir *via* a high voltage power supply (UltraVolt, Inc., South Thief River Falls, MN). This voltage scheme mitigated the potential drop across the islet chamber and ensured viability of the islets during two hours of experiments. The gate reservoir was grounded through a high voltage relay (Gigavac, Carpinteria, CA) during separations. In this condition, sample from the mixing channel was shunted to the waste channel by the flow from the gate channel. To perform an injection, the relay was floated to allow a small amount of sample into the separation channel. After 1 s, the gate reservoir was returned to ground and the injected mixture was separated with detection occurring at the end of the 1.5 cm separation channel. An injection was performed every 10 s.

A two-color laser-induced fluorescence detection system consisting of 488 and 635 nm laser lines with emission at 550 ± 40 nm and 675 ± 25 nm, respectively, was used as previously described.[28] Detection at 550 nm (green channel) was used to calibrate the perfusion system with fluorescein and detection at 675 nm (red channel) was used for detection of Cy5 labeled species in the separation channel. Control of injections and data collection were performed by a LabVIEW program.

Experimental protocol

Microfluidic devices were conditioned daily for at least 10 min each with 1 M NaOH, deionized water, and experimental buffers prior to the experiment. After experiments, the device was cleaned with deionized water for short term storage or 1 M NaOH and deionized water for long term storage. During all experiments, reservoirs were covered with plastic caps that had access holes for insertion of the platinum electrodes. A photograph of a microfluidic device with caps and electrodes is shown in the ESI,† Fig. S2.

Working solutions of Ab (150 nM) and Insulin* (150 nM) were prepared daily in a buffer that contained 25 mM tricine, 1 mM EDTA, 1 mg mL^{-1} BSA, 0.1% (w/v) Tween-20 and 40 mM NaCl, and the pH adjusted to 7.4 (TEAT40). Separation buffer consisted of 150 mM tricine and 20 mM NaCl with the pH adjusted to 7.4. For all experiments, the Ab and Insulin* reservoirs were filled with 90 μL of working solutions, and the gate and waste reservoirs were filled with 90 μL separation buffer. Calibration curves of the insulin immunoassay were obtained prior to islet experiments by placing insulin standards diluted in BSS (0–1500 nM) in the islet reservoir and measuring the ratio of the bound (B) and free (F) Insulin* (B/F). Throughout the remainder of the text, the concentrations of immunoassay reagents are referred to as the concentration in the fully mixed state, which assumes a 3-fold dilution of the concentrations in the microfluidic reservoirs.

Prior to islet experiments, islets were transferred into BSS containing 3 mM glucose and incubated for 30 min at 37 °C. The islet chamber was filled with pre-warmed BSS containing 3 mM glucose with the perfusion flow turned off. Islets were then hand loaded into the chamber using a micropipette. The perfusion flow rate was then resumed with 3 mM glucose for 5 min prior to the start of the experiments. Islets were checked for visible damage after each experiment. To maintain the temperature of the islet chamber at 37 °C, a thermofoil heater (Omega Engineering, Inc., Stamford, CT) was placed underneath the islet chamber and a thermocouple sensor was applied adjacent to the islet chamber on top of the device. A controller (Omega Engineering) was used to maintain the temperature at 36.5 ± 0.5 °C.

Data analysis

An automated program was used to determine the B/F from electropherograms using peak heights.[33] The average B/F from 25 consecutive electropherograms was calculated for each calibration point, and calibration curves were made by fitting a weighted four-parameter logistic function to the B/F ratios as a function of insulin concentration. Using the calibration curve, the limit of detection (LOD) was calculated by determining the concentration of insulin that would decrease the B/F ratio of a blank solution by an amount greater than three times the standard deviation of the blank. The insulin concentration that was secreted from islets was quantified based on the working calibration curve, converted to mass, and normalized to the perfusion flow rate.

The periodic nature of insulin secretion was assessed by performing a Fast Fourier transform on the data. All spectral analysis was performed on insulin secretion data without smoothing or detrending. In all figures of spectral analysis, the bottom x-axis details the frequency in Hz, while the top x-axis shows the equivalent period in minutes. A phase offset (ϕ_j) was calculated between each insulin and glucose oscillation by normalizing the difference in the times of each insulin oscillation peak ($t_{i,j}$) and the closest glucose oscillation peak ($t_{g,j}$) to the period of the glucose wave (T).[15,18]

$$\phi_j = \frac{360\left(t_{i,j} - t_{g,j}\right)}{T}$$

Results and discussion

In order to test the ability of islets to be entrained, physiological solutions of glucose need to be delivered to single or groups of islets. In the past, we have utilized a modified cell culture media containing different glucose levels for stimulating the release of insulin,[28] but wanted to move to a buffer system containing a physiologically relevant amount of Ca^{2+}. Calcium is a ubiquitous intracellular signal responsible for controlling numerous cellular processes[34] and its influx into β-cells is critical for the triggering of insulin secretion. Different buffers containing various levels of Ca^{2+} have been used to evoke insulin secretion from islets.[25,26] One of the advantages of the cell culture media is the low concentrations of divalent ions (*e.g.* Mg^{2+} and Ca^{2+}), which enables facile sampling of the islet chamber by EOF.[35]

A buffered saline solution, BSS, was chosen as the perfusion buffer because it contains a physiologically relevant Ca^{2+} concentration and mimics the extracellular ionic composition. However, we observed several problems when we initially moved to this buffer system. First, the shallow EOF channels would clog regularly, which was likely due to precipitation of $CaHPO_4$ and $CaCO_3$.[25] Tricine buffers have been shown to be effective for preventing precipitation,[27] and we modified the reagent and separation buffers to this buffer system. Second, because of the high ionic strength of the BSS, the sampling rate from the islet reservoir was low, which led to a high dilution of insulin in the mixing channel and reduced the sensitivity of the immunoassay.[26,36] To improve the sensitivity, the flow rates from the three immunoassay reservoirs (islet, Ab, and Insulin*) needed to be similar. To modify the flow rates, the distance from the islet chamber to the immunoassay mixing channel was decreased while increasing the ionic strength of the Ab and Insulin* buffers (Fig. 1). When the islet channel was 8 mm from the mixing channel and the ionic strength of the Ab and Ins* buffers was increased using 40 mM NaCl, the flow rates from the three reservoirs were approximately equal leading to better sensitivity in the immunoassay.

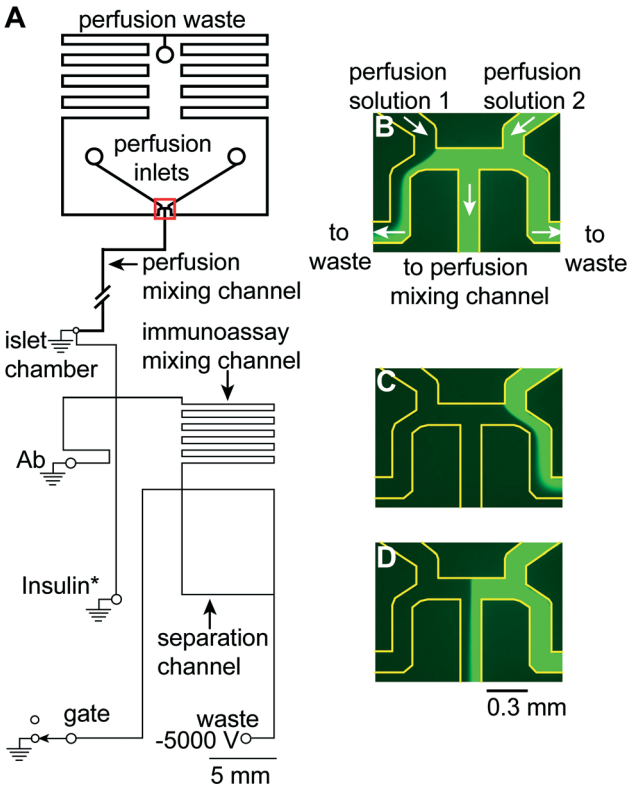

Fig. 1 Channel design of a microfluidic device to perfuse glucose waveforms to islets of Langerhans and monitor insulin secretion. (A) The perfusion channels, indicated by the thick lines, were 30 or 40 μm deep designed for gravity-driven perfusion of single or multiple islets, respectively. The perfusion mixing channel was 6 cm although for convenience, a shorter channel is shown as indicated by the break. The EOF channels, indicated by thinner lines, were 6 μm deep. The islet chamber was either 300 μm diameter to accommodate a single islet or 600 μm diameter to house 6–10 islets. (B–C) Images of the flow splitting junction (highlighted by the red rectangle in (A)) when fluorescein percentages beyond 100% (B) and beyond 0% (C) were perfused. Each of these images represents a condition where one of the perfusion media was completely diverted to the central perfusion mixing channel while the other was sent to perfusion waste. (D) A representative image of the junction when a percentage of fluorescein between 0 and 100% was perfused into the central perfusion mixing channel. The edges of all microfluidic channels in (B–D) are highlighted for clarity.

Characterization of the perfusion system

To test the hypothesis that glucose oscillations can entrain islets, it is necessary to have a perfusion system that can generate glucose waveforms. A gravity driven flow system has been developed to produce complex waveforms of sugar to force protein expression from yeast cells,[31,37] and we have used it to apply waveforms of glucose to synchronize $[Ca^{2+}]_i$ oscillations from groups of islets.[15] We made minor modifications to these previous systems for applying glucose waveforms to islets for measurement of insulin secretion (Fig. 1A). The perfusion system controlled the ratio of the two perfusion solutions, BSS with 3 and 13 mM glucose, that entered the perfusion mixing channel. Because the perfusion mixing channel led directly to the islet chamber, this ratio dictated

the glucose concentration delivered to the islet chamber. The ratio was determined by the flow rates of the two solutions which were controlled by an automated system that used a stepper motor to control the height of one perfusion syringe, while a belt and pulley ensured the other perfusion syringe moved in an equal, but opposite, direction. In this way, as the flow rate of one increased, the other decreased in an equal amount and the total flow rate remained constant.

The fluid directions of the two perfusion solutions are shown by the white arrows in Fig. 1B, which is a zoomed in view of the region highlighted by the red box in Fig. 1A. The two perfusion solutions entered the device and met at a flow-splitting junction. There were then three outlets for the solutions to leave this junction. The center was the perfusion mixing channel which led directly to the islet chamber. The other two outlets, one on each side of the perfusion mixing channel, were tied together at the perfusion waste. The flow rates of the two input solutions dictated the position of the two streams and therefore the amount of each that was sent to the perfusion mixing channel.

To help in visualizing the flows, 100 μM fluorescein was added to the second perfusion reservoir and the flow-splitting region was imaged with a CCD camera. Fig. 1B shows the positions of the two solutions when the flow rate from the first perfusion solution was low and the other solution was high. The first solution was shunted to waste while 100% of the second solution was sent to the perfusion mixing channel. In contrast, Fig. 1C shows the flows in the opposite case where 0% of the second solution was delivered to the perfusion mixing channel. Fig. 1D shows a situation where 55% of the second solution was delivered to the perfusion mixing channel. Some of the benefits of this perfusion system include the non-pulsatile flow rates since hydrostatic pressure was used, and that neither of the flows had to be stopped, even at the extremes of 0 and 100%. This eliminated any back diffusion of the solutions into each other and eliminated pressure pulses from starting or stopping the flows. More information on how the perfusion system was calibrated is provided in the ESI† (Fig. S1), as well as a movie of the perfusion solutions moving with the corresponding changes in the position of the flow streams (Movie S1†).

The major modification to this perfusion system for use in stimulating islets for entrainment of hormone secretion was that the perfusion mixing channel was increased to 6 cm to allow for complete mixing of the two perfusion solutions (Fig. 1A). Initially, the mixing channel was folded to conserve space on the device; however, this resulted in the mixing channel being in close proximity to the islet chamber. Because of the increased temperature near the islet chamber required to maintain a physiological environment, and the large effect of temperature on solution viscosity, variations in the perfusion flow rates were observed resulting in irreproducible flow. To minimize this effect, the perfusion mixing channel was extended, minimizing the length of the channel that was exposed to the elevated temperature near the islet chamber.

Both the entrainment of insulin secretion from single and groups of islets are important for the initial testing of the hypothesis that oscillatory glucose levels may synchronize insulin output.[14] To accommodate detection of both low and high concentrations of insulin secretion from single and groups of islets, islet chamber sizes as well as the perfusion channel dimensions were modified for different applications. A 300 μm diameter islet chamber with a 30 μm deep perfusion channel was used for the measurement of insulin secretion from a single islet.

The flow rate to the islet chamber was measured by perfusing fluorescein and recording the time for the change in the fluorescence signal to be detected at the inlet of the islet chamber. The time was 67.5 ± 0.4 s (n = 8) indicating a flow rate of 0.22 ± 0.05 μL min^{-1}. More details on how the flow rate was measured are provided in the ESI.† For the monitoring of insulin secretion from multiple islets, a 600 μm diameter islet chamber with a 40 μm deep perfusion channel was used. With the same height of the perfusion syringes, a flow rate of 0.44 ± 0.05 μL min^{-1} was generated. This higher flow rate diluted the secreted insulin from groups of islets into the dynamic range of the calibration curve. It should be pointed out that higher flow rates have been used for inducing oscillations of $[Ca^{2+}]_i$ and/or insulin release from islets with no evidence of shear-induced damage.[18,25–28,38,39] If shear forces were problematic, other geometries for islet perfusion could be used.[40]

Characterization of the combined perfusion and separation system was performed by delivering insulin to the islet chamber using the perfusion system, sampling the insulin from the islet chamber using EOF, followed by online mixing with the immunoassay reagents. Injection and separation cycles were performed every 10 s and the resulting B/F was monitored as the insulin concentration delivered to the islet chamber was varied. Fig. 2A shows the monitored B/F (black trace) when step changes of insulin (red trace) were perfused. When a new concentration of insulin was delivered to the islet chamber, the B/F reached a new plateau in less than 8 runs indicating a response time of ~80 s. There was a slight drift of the B/F at each calibration point shown in Fig. 2A. This was likely due to non-specific adsorption of immunoassay reagents, solution evaporation, or a change in the pH in the reservoirs during the course of the experiments. However, these effects were relatively small as indicated by the high precision of the B/F ratios (RSD from 2–8% for all calibration points tested). The RSDs of the migration times of the bound and free Insulin* peaks were ~1% indicating highly reproducible flow rates in the device. Fig. 2B is the calibration curve that was obtained by plotting the average B/F against the perfused insulin concentrations and the detection limit was calculated to be 3 nM. The RSD of the calibration points ranged from 2–8% indicating a stable response.

In Fig. 2A, the changes in the insulin B/F ratios lagged the perfused insulin step changes. This lag included the time for the perfusion solution to travel from the splitting junction to

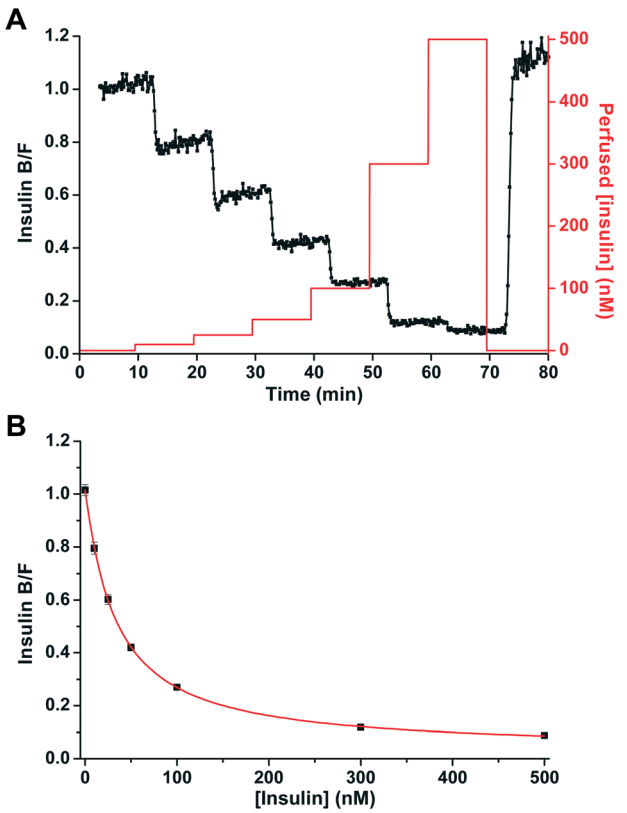

Fig. 2 Characterization of the combined perfusion and separation system. (A) The measured insulin B/F (left *y* axis, black trace) when step changes of insulin (right *y* axis, red trace) were perfused into the islet chamber and sampled by EOF. (B) The average insulin B/F ratios measured in (A) were plotted against the perfused insulin concentrations. Error bars indicate ±1 standard deviation.

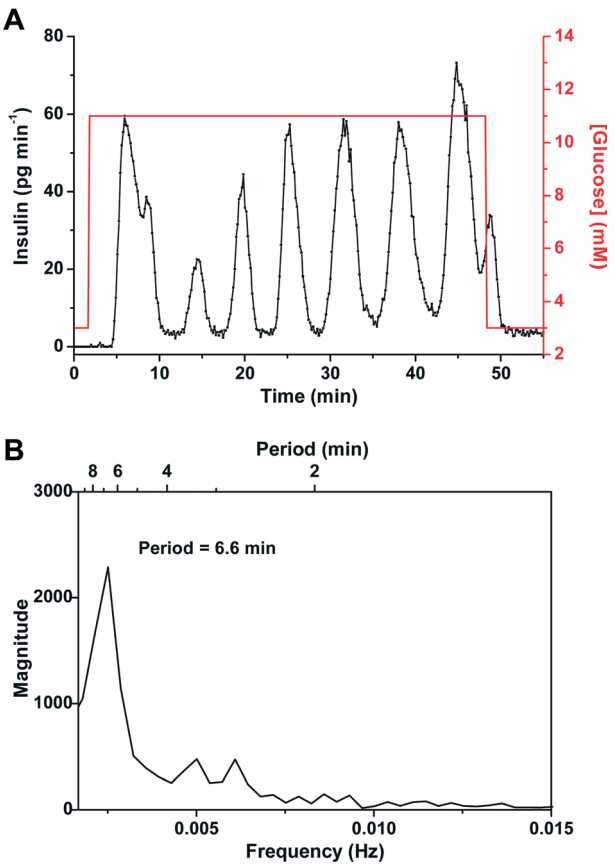

Fig. 3 Pulsatile insulin secretion from single islets at constant glucose levels. (A) A representative example of insulin oscillations (black trace, left *y* axis) from a single islet monitored as the glucose concentration (red line, right *y* axis) was increased from 3 to 11 mM. The islet was perfused with BSS at 0.22 μL min^{-1}. (B) Spectral analysis of the pulsatile insulin secretion data from 4–48 min when the islet was perfused with 11 mM glucose showing a major peak at 6.6 min.

the islet chamber and the time it took for the sample to travel from the islet chamber to the detection point in the separation channel. In the data shown in Fig. 2A, the lag time was 3.2 min. The lag time was measured for each device (ranged from 3.2 to 4.4 min) and used to correct all insulin secretion profiles shown.

Monitoring insulin secretion from single islets at constant glucose level

The first step towards the use of this system for entraining islets is to confirm that it can be used to measure pulsatile insulin secretion from single islets at constant glucose. Single islets were perfused with a step change of glucose from 3 to 11 mM in BSS while insulin secretion continuously monitored. Fig. 3A shows a representative example of the profiles measured from single islets (n = 4). As can be seen, the insulin levels measured were clearly oscillatory during perfusion with 11 mM glucose. Fig. 3B is a spectral analysis of the secretion data during the period that the islet was exposed to 11 mM glucose and it shows a dominant peak at a period of 6.6 min. All tested islets (n = 4) exhibited similar oscillatory insulin release profiles and the secretion amounts and oscillation periods were in agreement with previously reported values.[26,41] As a control experiment, the 13 mM glucose perfusion solution was replaced with 3 mM glucose containing 100 nM fluorescein. Insulin secretion was monitored while the heights of the perfusion syringes were changed. Insulin secretion was undetectable during the course of the experiment indicating that movement of the perfusion syringes or fluorescein was not inducing insulin release (Fig. S3†).

Entrainment of insulin secretion from single islets to oscillatory glucose levels

After successful monitoring of pulsatile insulin secretion, this system was used to test the entrainment of single islets to glucose waveforms. Fig. 4A details the experimental procedure where after a 5 min perfusion with 3 mM glucose, the glucose concentration was increased to 11 mM inducing insulin secretion. At 32 min, the glucose concentration was made to oscillate around a mean of 11 mM with a period of 5 min and amplitude of 2 mM. After 25 min, the phase of the sinusoidal wave was switched 180° to disrupt the entrainment and determine if the islet could be entrained again to the glucose wave.

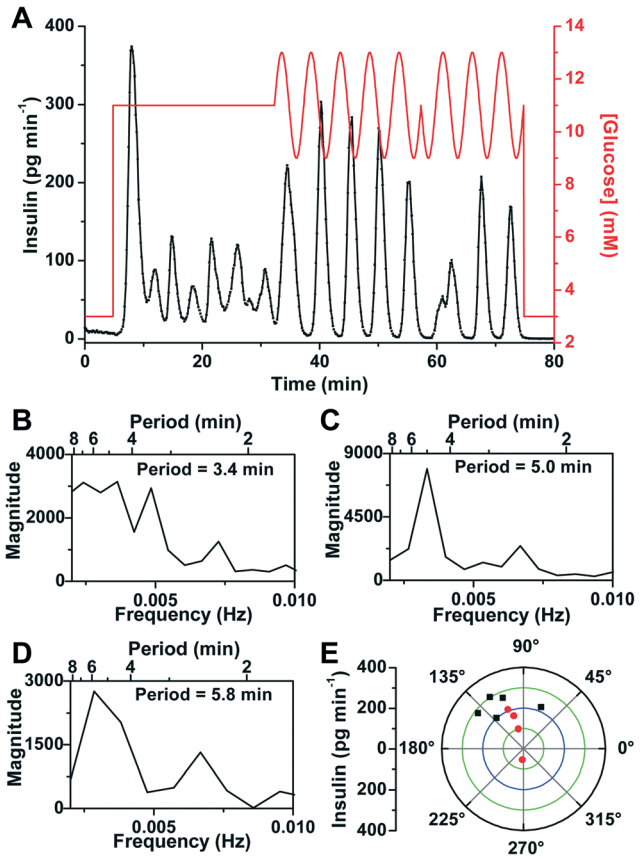

Fig. 4 Entrainment of insulin secretion from single islets to an oscillatory glucose level. (A) Glucose was raised from 3 mM to 11 mM to induce oscillatory insulin secretion from a single islet. The glucose concentration was then made to oscillate around a mean of 11 mM with a period of 5 min and amplitude of 2 mM. After 25 min, a 180° phase shift was introduced to the sinusoidal glucose wave. (B–D) Spectral analysis of the data in (A) when the islet was perfused with (B) constant 11 mM glucose from 5–32 min, (C) oscillatory glucose with a period of 5 min from 32–57 min, and (D) oscillatory glucose with a period of 5 min from 57–75 min after the 180° phase shift. (E) Phase angles of the insulin pulses to the glucose waves on a polar plot where the amplitude of insulin is indicated by the radial distance. The black points show phase angles when the islet was perfused with sinusoidal glucose waves with a period of 5 min from 32–57 min and red points indicate phase angles after the 180° phase shift in glucose (57–75 min).

To help determine if the islet was entrained to the glucose wave, spectral analysis of the insulin secretion data was performed during each of these segments. It is expected that the islet would shift its secretion period to the applied forcing period if it was entrained. During exposure to the constant 11 mM glucose, the insulin oscillated with a period of 3.4 min (Fig. 4B). During the delivery of the sinusoidal glucose wave, the insulin secretion pulse period was 5.0 min (Fig. 4C) while after the 180° phase shift in glucose, the period was 5.8 min (Fig. 4D). The periods found by the spectral analysis were not exactly what were applied by the perfusion system because the insulin pulses are not perfectly sinusoidal, noise was present in the data, and the sampling frequency limits the frequency resolution. We have also observed that entrainment of $[Ca^{2+}]_i$ oscillations required approximately one oscillation period for entrainment,[17,18] but the data in Fig. 4A was analyzed using the entire time of the applied glucose wave. Nevertheless, the shifting of the islet pulse period from its natural period (3.4 min) to that of the forcing period is a good indicator that the islet was entrained.

To visualize how the islet became entrained during the application of the sinusoidal glucose wave, the phase angles between each insulin and glucose oscillation were measured. For an entrained system, the phase angles should remain constant with minimal phase slipping.[15,18,42] Fig. 4E shows the phase angle measured between each insulin and glucose oscillation on a polar plot where the amplitude of the insulin oscillation is indicated by the distance from the radius. The black data points on Fig. 4E represent the phase of the insulin oscillations to the glucose oscillations during the period from 32 to 57 min, or prior to the 180° glucose shift. The first oscillation was 67° lagging the glucose oscillation, while the next four points were in a narrow range between 112–142°. These results indicated that the islet took approximately one oscillation period to adjust to the glucose wave, but then phase locked to the sinusoidal glucose wave. The red points on the polar plot are a measure of the phase after the 180° shift in the glucose wave. These values are within the range of the initial points except for the first point, at an angle of 270°, that occurred when the insulin oscillation was adjusting to the phase shift. The convergence of the phases into a narrow range indicated successful entrainment of the insulin secretion.[15,42]

Fig. 5A is another example in which the glucose concentration was made to oscillate with a period of 5 min followed by a 180° phase shift, but in this experiment, the glucose oscillation period was then increased to 10 min. The insulin secretion initially oscillated with a period of 4.0 min (Fig. 5B) during constant glucose. During exposure to the 5 min glucose wave, the islet shifted its secretion period to 5.0 min (Fig. 5C). After the 180° phase shift and an increase of the glucose wave period to 10 min, the islet followed the new glucose wave by changing its oscillation period to 10.0 min (Fig. 5D). The phase of each insulin oscillation to the glucose oscillations are shown in Fig. 5E with the 5 min waves shown by the black points and the 10 min waves shown by the red points. Again, the phase of the first insulin oscillation after exposure to the oscillatory glucose level was shifted from the remaining phases measured. Immediately after the application of the 10 min glucose wave, the secretion locked into a range from 42–62°.

The results of all tested islets (n = 3) showed that upon application of a glucose sinusoidal wave, insulin secretion was entrained to the forcing period. Application of a different glucose oscillation period reset the insulin oscillation to this new period. All of these observations clearly demonstrated the successful entrainment of insulin oscillations by the forcing glucose waveforms. Interestingly, in most cases, the oscillatory glucose level induced larger amplitude insulin oscillations compared with the constant glucose concentration.

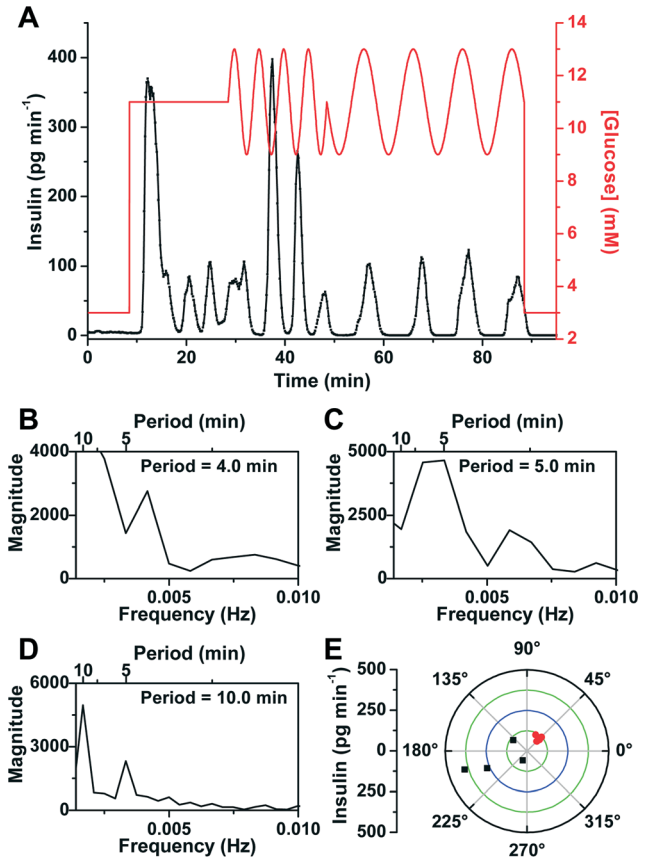

Fig. 5 Entrainment of insulin secretory oscillations from single islets to different period glucose waves. (A) A representative trace of insulin secretion from a single islet when it was exposed to a glucose signal with periods of 5 and 10 min. (B–D) Spectral analysis of the data in (A) when the islet was perfused with (B) a constant 11 mM glucose from 8–28 min, (C) oscillatory glucose levels with a period of 5 min from 28–48 min, and (D) oscillatory glucose levels with a period of 10 min from 48–88 min. (E) Amplitude of insulin oscillations plotted against phase angles between each insulin and glucose oscillation. Black and red points indicate phase angles of each oscillation during exposure to glucose oscillations with periods of 5 and 10 min, respectively.

Although we are unsure why this occurs, this effect has not been observed in the entrainment of oscillations in $[Ca^{2+}]_i$.[15–18]

Synchronization of insulin secretion from multiple islets

We next used this system to determine if insulin secretion from multiple islets can be synchronized to an external glucose stimulus. As shown in Fig. 3A, 4A, and 5A, single islets secrete insulin in pulses during constant glucose, but if these islets were placed together in a single chamber, and the insulin signal was measured, these pulses would overlap resulting in an elevated but constant level of insulin.[14] Upon application of an oscillatory glucose wave, all islets should entrain to the forcing period and the average secretion should display a pulsatile pattern with a similar period to the forcing glucose wave.[17]

To test if synchronization of insulin release occurs, groups of 6–10 islets were placed in a 600 μm islet chamber and a constant 11 mM glucose was applied followed by a sinusoidal wave with a period of 5 min and an amplitude of 2 mM. Fig. 6A shows a representative trace of the insulin release taken from a group of 10 islets. When the glucose concentration was changed from 3 to 11 mM, a burst of insulin secretion was observed that decreased slowly, but no oscillations were observed. We expect that this was due to the individual islets oscillating at different frequencies and being out of phase resulting in a constant insulin level detected.[17] When the sinusoidal glucose wave was applied, an overall oscillatory insulin profile was observed with a period of 5.0 min (Fig. 6B) indicating that the islets were synchronized. As seen in Fig. 6C, a narrow range (128–184°) of the phase between the insulin and glucose oscillations indicated entrainment to the external glucose signal. The relative magnitude of the insulin oscillations shown in Fig. 6 is lower compared to the relative magnitude of single islet oscillations. This could be due to a fraction of the 10 islets being synchronized, or it could be due to non-perfect synchronization of all islets. Because we cannot measure secretion from each individual islet, it is impossible to know which of these two possibilities occurred. However, we believe that it is impractical for the insulin pulses from each islet to be perfectly aligned to give baseline resolved pulses since they could have different amplitudes, slightly different frequencies, or even have different peak shapes. A similar result was observed when monitoring oscillations of $[Ca^{2+}]_i$ from groups

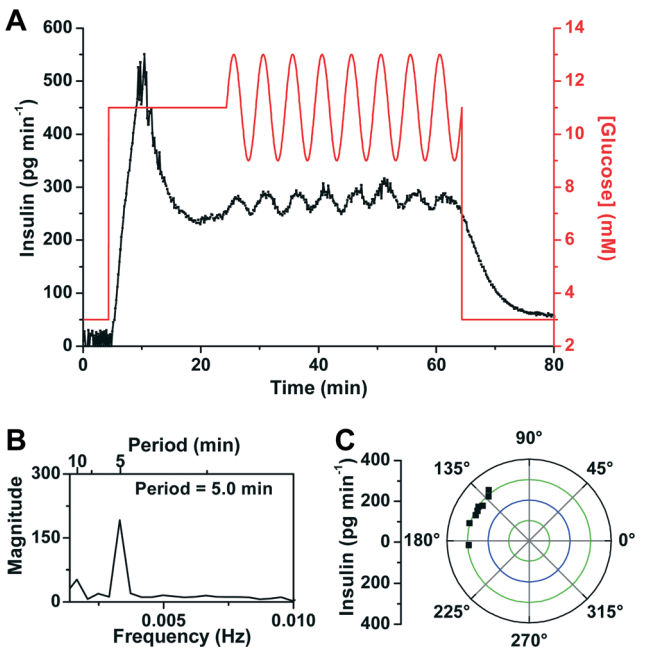

Fig. 6 Synchronization of insulin secretion from multiple islets. (A) A representative example of the insulin secretion profile measured from a group of 10 islets when the glucose concentration was held at a constant 11 mM followed by oscillations with a period of 5 min and amplitude of 2 mM. (B) Spectral analysis of insulin secretion when islets were perfused with oscillatory glucose waves from 24–64 min showing a major peak at 5.0 min. (C) Phase angles between each insulin and glucose oscillations from the data in (A).

of islets exposed to an oscillatory glucose level; although all islets were entrained, the averaged $[Ca^{2+}]_i$ from all of these islets was relatively low in magnitude compared to a single islet exposed to an oscillatory glucose level.[17]

In all experiments (n = 10), insulin measured from groups of islets was not oscillatory during exposure to constant glucose, while oscillatory insulin release was observed when the glucose level was made to oscillate. These data suggest that insulin secretion from multiple islets were entrained and synchronized, and demonstrate the utility of this system for testing synchronization of islets and the potential use of it in mechanistic studies of oscillatory insulin release.

Conclusions

We have described a microfluidic system that can generate glucose waveforms to stimulate islets while allowing high temporal resolution monitoring of insulin secretion. This system was applied to study entrainment and synchronization of oscillatory insulin secretion from single and multiple islets to forcing glucose waveforms and is expected to provide a powerful technique to understand the underlying mechanism of oscillatory insulin secretion observed *in vivo*. The method developed here is easily amenable to coupling with fluorescent cell imaging methods to investigate intracellular signal transduction pathways simultaneously with insulin secretion. The system can be used to measure other peptides released from islets or used with other cell types by altering the immunoassay reagents, making this a versatile tool for cell biology.

Acknowledgements

This work was supported by National Institutes of Health grant DK080714. We would like to thank Professor Stephen Weber and Juanfang Wu for the help in simulations of flow-gated injections at high ionic strengths.

References

1 K. Tornheim, *Diabetes*, 1997, **46**, 1375–1380.
2 R. Bertram, L. Satin, M. Zhang, P. Smolen and A. Sherman, *Biophys. J.*, 2004, **87**, 3074–3087.
3 M. A. Ravier, M. Guldenagel, A. Charollais, A. Gjinovci, D. Caille, G. Sohl, C. B. Wollheim, K. Willecke, J. C. Henquin and P. Meda, *Diabetes*, 2005, **54**, 1798–1807.
4 J. V. Rocheleau, M. S. Remedi, B. Granada, W. S. Head, J. C. Koster, C. G. Nichols and D. W. Piston, *PLoS Biol.*, 2006, **4**, e26.
5 C. S. Mao, N. Berman, K. Roberts and E. Ipp, *Diabetes*, 1999, **48**, 714–721.
6 C. S. Nunemaker, M. Zhang, D. H. Wasserman, O. P. McGuinness, A. C. Powers, R. Bertram, A. Sherman and L. S. Satin, *Diabetes*, 2005, **54**, 3517–3522.
7 C. S. Nunemaker, D. H. Wasserman, O. P. McGuinness, I. R. Sweet, J. C. Teague and L. S. Satin, *Am. J. Physiol.*, 2006, **290**, E523–E529.
8 N. Porksen, M. Hollingdal, C. Juhl, P. Butler, J. D. Veldhuis and O. Schmitz, *Diabetes*, 2002, **51**(Suppl 1), S245–S254.
9 A. V. Matveyenko, D. Liuwantara, T. Gurlo, D. Kirakossian, C. Dalla Man, C. Cobelli, M. F. White, K. D. Copps, E. Volpi, S. Fujita and P. C. Butler, *Diabetes*, 2012, **61**, 2269–2279.
10 S. O'Rahilly, R. C. Turner and D. R. Matthews, *N. Engl. J. Med.*, 1988, **318**, 1225–1230.
11 O. Schmitz, N. Porksen, B. Nyholm, C. Skjaerbaek, P. C. Butler, J. D. Veldhuis and S. M. Pincus, *Am. J. Physiol.*, 1997, **272**, E218–E226.
12 J. Sturis, W. L. Pugh, J. Tang, D. M. Ostrega, J. S. Polonsky and K. S. Polonsky, *Am. J. Physiol.*, 1994, **267**, E250–E259.
13 P. Gilon, M. A. Ravier, J. C. Jonas and J. C. Henquin, *Diabetes*, 2002, **51**(Suppl 1), S144–S151.
14 M. G. Pedersen, R. Bertram and A. Sherman, *Biophys. J.*, 2005, **89**, 107–119.
15 R. Dhumpa, T. M. Truong, X. Wang, R. Bertram and M. G. Roper, *Biophys. J.*, 2014, **106**, 2275–2282.
16 M. G. Pedersen, E. Mosekilde, K. S. Polonsky and D. S. Luciani, *Biophys. J.*, 2013, **105**, 29–39.
17 X. Zhang, A. Daou, T. M. Truong, R. Bertram and M. G. Roper, *Am. J. Physiol.*, 2011, **301**, E742–E747.
18 X. Zhang, A. Grimley, R. Bertram and M. G. Roper, *Anal. Chem.*, 2010, **82**, 6704–6711.
19 R. A. Ritzel, J. D. Veldhuis and P. C. Butler, *Am. J. Physiol.*, 2006, **290**, E750–E756.
20 J. Sturis, E. Van Cauter, J. D. Blackman and K. S. Polonsky, *J. Clin. Invest.*, 1991, **87**, 439–445.
21 B. Hellman, A. Salehi, E. Gylfe, H. Dansk and E. Grapengiesser, *Endocrinology*, 2009, **150**, 5334–5340.
22 S. H. Song, S. S. McIntyre, H. Shah, J. D. Veldhuis, P. C. Hayes and P. C. Butler, *J. Clin. Endocrinol. Metab.*, 2000, **85**, 4491–4499.
23 B. Hellman, *Upsala J. Med. Sci.*, 2009, **114**, 193–205.
24 M. G. Roper, J. G. Shackman, G. M. Dahlgren and R. T. Kennedy, *Anal. Chem.*, 2003, **75**, 4711–4717.
25 J. G. Shackman, G. M. Dahlgren, J. L. Peters and R. T. Kennedy, *Lab Chip*, 2005, **5**, 56–63.
26 J. F. Dishinger, K. R. Reid and R. T. Kennedy, *Anal. Chem.*, 2009, **81**, 3119–3127.
27 K. R. Reid and R. T. Kennedy, *Anal. Chem.*, 2009, **81**, 6837–6842.
28 A. R. Lomasney, L. Yi and M. G. Roper, *Anal. Chem.*, 2013, **85**, 7919–7925.
29 C. Guillo, T. M. Truong and M. G. Roper, *J. Chromatogr. A*, 2011, **1218**, 4059–4064.
30 X. Wang and M. G. Roper, *Anal. Methods*, 2014, **6**, 3019–3024.
31 M. S. Ferry, I. A. Razinkov and J. Hasty, *Methods Enzymol.*, 2011, **497**, 295–372.
32 S. C. Jacobson, S. V. Ermakov and J. M. Ramsey, *Anal. Chem.*, 1999, **71**, 3273–3276.
33 J. G. Shackman, C. J. Watson and R. T. Kennedy, *J. Chromatogr. A*, 2004, **1040**, 273–282.
34 M. J. Berridge, P. Lipp and M. D. Bootman, *Nat. Rev. Mol. Cell Biol.*, 2000, **1**, 11–21.

35 S. Datta, A. T. Conlisk, H. F. Li and M. Yoda, *Mech. Res. Commun.*, 2009, **36**, 65–74.
36 J. G. Shackman, K. R. Reid, C. E. Dugan and R. T. Kennedy, *Anal. Bioanal. Chem.*, 2012, **402**, 2797–2803.
37 F. Menolascina, G. Fiore, E. Orabona, L. De Stefano, M. Ferry, J. Hasty, M. di Bernardo and D. di Bernardo, *PLoS Comput. Biol.*, 2014, **10**, e1003625.
38 L. A. Godwin, M. E. Pilkerton, K. S. Deal, D. Wanders, R. L. Judd and C. J. Easley, *Anal. Chem.*, 2011, **83**, 7166–7172.
39 J. V. Rocheleau, G. M. Walker, W. S. Head, O. P. McGuinness and D. W. Piston, *Proc. Natl. Acad. Sci. U. S. A.*, 2004, **101**, 12899–12903.
40 P. N. Silva, B. J. Green, S. M. Altamentova and J. V. Rocheleau, *Lab Chip*, 2013, **13**, 4374–4384.
41 N. Porksen, *Diabetologia*, 2002, **45**, 3–20.
42 A. Jovic, B. Howell, M. Cote, S. M. Wade, K. Mehta, A. Miyawaki, R. R. Neubig, J. J. Linderman and S. Takayama, *PLoS Comput. Biol.*, 2010, **6**, e1001040.

